High-Q optomechanical GaAs nanomembranes

Liu, Jin; Usami, K.; Naesby, A.; Bagci, T.; Polzik, E.S.; Lodahl, P.; Stobbe, S.

Published in:
Applied Physics Letters

Link to article, DOI:
10.1063/1.3668092

Publication date:
2011

Document Version
Publisher's PDF, also known as Version of record

High-Q optomechanical GaAs nanomembranes

J. Liu, K. Usami, A. Naesby, T. Bagci, E. S. Polzik et al.

Citation: Appl. Phys. Lett. **99**, 243102 (2011); doi: 10.1063/1.3668092
View online: http://dx.doi.org/10.1063/1.3668092
View Table of Contents: http://apl.aip.org/resource/1/APPLAB/v99/i24
Published by the American Institute of Physics.

High-Q optomechanical GaAs nanomembranes

J. Liu,[1,2,a)] K. Usami,[3] A. Naesby,[3] T. Bagci,[3] E. S. Polzik,[3] P. Lodahl,[2] and S. Stobbe[2]
[1]*DTU Fotonik, Department of Photonics Engineering, Technical University of Denmark, Ørsteds Plads 343, DK-2800 Kgs. Lyngby, Denmark*
[2]*Niels Bohr Institute, University of Copenhagen, Blegdamsvej 17, DK-2100 Copenhagen, Denmark*
[3]*QUANTOP – Danish National Research Foundation Center for Quantum Optics, Niels Bohr Institute, University of Copenhagen, Blegdamsvej 17, DK-2100 Copenhagen, Denmark*

(Received 2 October 2011; accepted 18 November 2011; published online 12 December 2011)

We demonstrate that suspended single-crystal GaAs nanomembranes exhibit mechanical Q-factors exceeding 2×10^6 at room temperature, which makes them a very promising platform for optomechanics. Because of the completely removed substrate and their millimeter-scale lateral size, the membranes can be incorporated in macroscopic optical cavities for quantum optomechanics experiments. We have measured the mechanical mode spectrum and spatial profiles and find good agreements with theory. Our work paves the way for optomechanical experiments with direct band gap semiconductors in which not only radiation pressure but also other mechanisms involving embedded light emitters could be exploited for quantum optical control of massive mechanical systems. © *2011 American Institute of Physics*. [doi:10.1063/1.3668092]

Quantum optomechanics has become an emerging field with the goal of engineering and detecting quantum states of massive mechanical systems such as the quantum ground state[1,2] or entangled quantum states.[3,4] In this rapidly expanding field, various materials and geometries are being pursued, in order to control the coupling between phonons and photons.[5–7]

Incorporating direct band gap semiconductor materials in optomechanics exhibits unexplored prospects due to a number of advantageous properties. In particular, GaAs enables the integration of optoelectronic functionality with nanomechanical elements.[8] The noncentrosymmetric nature of the zinc-blende crystal structure of GaAs results in an appreciable piezoelectric coefficient, enabling efficient actuation or transduction.[9] Furthermore, there is a proposal of cooling the lattice temperature of semiconductors down to 10 K, referred to as optical refrigeration, although experimental demonstrations have not yet been realized.[10] Quantum dots embedded in GaAs also enable strong coupling between a photon and a confined exciton.[11] Much effort has been invested in fabricating GaAs-based micro-resonators[12,13] and improving their mechanical properties by strain engineering.[14] Coupling the intrinsic physical properties of direct band gap semiconductors to mechanical modes would enable a multitude of effects within cavity quantum optomechanics engineering.[15] Very recent results on both GaAs disk resonators and InP photonic crystal cavities show the feasibility of realizing optomechanical systems in direct band gap semiconductors,[16–18] but it is widely observed that GaAs microresonators suffer from low Q-factors, which limit the optomechanical cooling performance. Here, we present the experimental realization of millimeter sized single-crystal GaAs nanomembranes with extremely high-Q factors that have very promising applications.

The GaAs membrane is fabricated from a GaAs/AlGaAs heterostructure wafer comprised of a (100)-oriented GaAs substrate (thickness: 350 μm), $Al_{0.85}Ga_{0.15}As$ etch stop layer (thickness: 1 μm), and a GaAs capping layer (thickness: 160 nm), which is shown in Fig. 1(a). The first step is to remove the substrate with selective citric acid wet-etching by using AlGaAs as an etch stop layer.[19] Then a non-buffered hydrofluoric acid (HF (10%)) selective wet-etching follows in order to remove the AlGaAs sacrificial layer.[20] The single-crystal nanomembranes made by our method are optically accessible from both sides, which enables implementing cavity optomechanical cooling schemes.

The detailed fabrication process is as follows: photoresist (AZ 5214E) with a thickness of 3 μm is coated on both sides of the wafer and the patterns of the holes with different diameters ranging from 500 μm to 1 mm are defined by photolithography. After 30 min hard baking at a temperature of 140 °C on a hotplate, the wafer is immersed into citric acid/H_2O_2 solution (4 citric acid (50% by wt.)/1 H_2O_2 (30%))[19] with magnetic stirring for 20 h to etch through the GaAs substrate. Thanks to the excellent etch rate selectivity for GaAs versus AlGaAs in the citric acid/H_2O_2 solution, the 160 nm GaAs layer is intact due to the protection of the AlGaAs layer and the photoresist during the citric acid wet-etching.

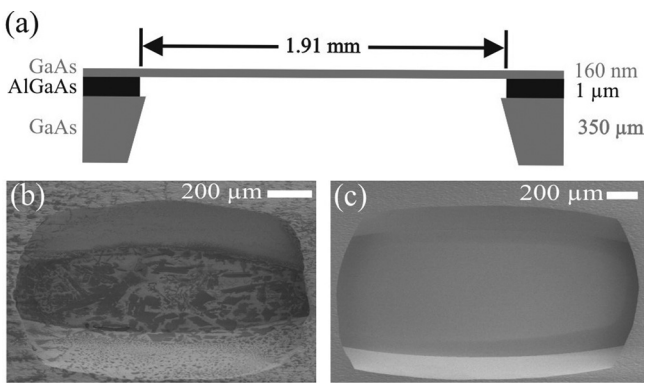

FIG. 1. (a) A cross section sketch of the nanomembrane. (b) SEM of the backside of the nanomembrane before and (c) after the cleaning processes.

[a)]Electronic mail: jinl@fotonik.dtu.dk.

Once the substrate is etched away, another selective wet-etching follows to remove the AlGaAs sacrificial layer and finally a GaAs nanomembrane is formed after removing the photoresist.

We have observed that often a thin layer of photoresist and submicron-sized particles are left after the completion of photoresist removal, which is shown by the scanning electron micrograph (SEM) in Fig. 1(b). These residues can be significant sources of light scattering and deteriorations of mechanical Q-factors. The remnant resist can only be removed by oxygen plasma, while the submicron-sized particles speculated to be hydroxide of aluminium[21] can be removed in potassium hydroxide (KOH) solutions. Figure 1(c) shows SEM of a nanomembrane after the oxygen plasma and KOH (25 g/100 ml deionized water) cleaning processes. We found that the shapes of the fabricated nanomembranes deviated significantly from the circular photolithography masks. This comes from the different etch rates for different crystallographic planes of GaAs in citric acid. A close inspection of the membranes reveals that they are not completely flat, but rather they are bowing with an amplitude at the center of the membranes on the order of a few microns. The size of the largest nanomembrane made by our method is roughly 1.36 mm in width and 1.91 mm in length.

We have characterized the mechanical properties of the nanomembranes via frequency noise spectrum by using cavity transmission measurements. A dielectric concave mirror and a 160-nm-thick GaAs membrane form a cavity with the measured finesse of about 10. By feeding the spectrum analyzer with the RF signal from the photodiode, we have observed 14 resonance frequencies ranging from 17.5 kHz to 59.5 kHz, see Fig. 2(a). The observed resonance frequencies conform within roughly 10% to the vibrational modes of a taut rectangular drumhead,[22] where the resonance frequency for the (m,n)-mode is given by $\nu_{m,n} = \sqrt{\frac{T}{4\rho}\left(\left(\frac{m}{L}\right)^2 + \left(\frac{n}{W}\right)^2\right)}$ with a membrane mass density $\rho = 5.36$ g/cm and a tensile stress T as a fitting parameter (the resultant T is 7 MPa), where L and W are the length and width of the membrane, respectively. The Q-factor is defined as $Q = \omega/\Gamma$, where $\nu = \omega/2\pi$ is the resonance frequency and Γ is the mechanical damping rate. Γ is measured through a ringdown measurement in which the ringdown of the mechanical modes is observed by inducing the oscillations with an intensity-modulated cavity field. A typical ringdown measurement for the (4,3)-mode is shown in the inset of Fig. 2(b). Due to the optomechanical effect,[5–7] the Q-factors and resonance frequencies vary with input powers in the ringdown measurements. The intrinsic mechanical Q-factors are extracted from the power-dependent ringdown measurements by extrapolating the Q-factors to zero cavity input power. Since the damping rate of a mechanical mode (i.e., inverse of Q) generally scales linearly with ν, $Q \times \nu$ is an important parameter for the mechanical characterizations. Table I lists the resonance frequencies, the corresponding Q-factors, and the product of Q and ν for the modes we have carefully characterized. The highest Q-factor of 2.3×10^6 and $Q \times \nu$ value of 1.4×10^{11}, which is comparable to the state-of-the-art values for GaAs resonators (cf. Refs. 13, 16, and 17), are found for the (4,3)-mode ($\nu = 59.5$ kHz). We stress that much higher Q-factors for our GaAs nanomembranes are expected at cryogenic temperatures.

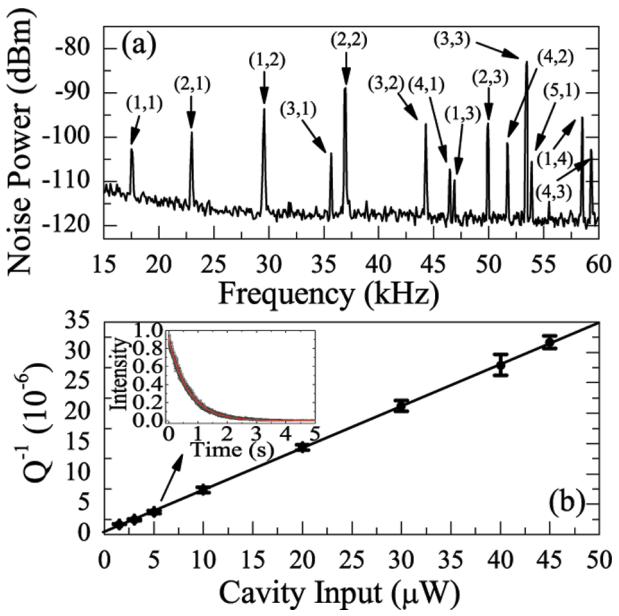

FIG. 2. (Color online) (a) Measured frequency noise spectrum in the 10 kHz-60 kHz range presenting a series of peaks corresponding to the different mechanical modes labeled by the mode numbers in the parentheses. (b) Inverse Q-factor of the (4,3)-mode for different cavity input powers, the points are measurement data and the line is produced by a least-square linear fit. Inset: ringdown measurement with a cavity input power of 5 μW.

The vibration amplitudes, which are proportional to the vibration speeds for a given resonance frequency, are mapped by a laser-Doppler vibrometer [MSA-500 Micro System Analyzer (Polytec Ltd.)] with a white light interferometry method. Due to space limitations in the experimental method, these measurements were performed on a smaller sample (roughly 0.7 mm by 1.4 mm) than the one presented in Fig. 1(c). The vibration profiles of the (1,1), (2,1), (1,3), and (2,2)-modes are shown on the left-hand side of Fig. 3 while the normalized vibration amplitudes of a taut rectangular drumhead ($a_{m,n}(x,y) = \sin(\frac{\pi m x}{L})\sin(\frac{\pi n y}{W})$ for the (m,n)-mode) are on the right-hand side. We find a good agreement between the measured mechanical mode profiles and the calculation. This model is also used to estimate the fundamental resonance frequency. The internal stress of the $Al_xGa_{1-x}As$/GaAs interface due to the lattice mismatch during growth can be approximated as[23] $133 \times x$ and in our case $x = 0.85$. Thus, a tensile stress T of 110 MPa is predicted, which leads to a fundamental resonance frequency (the (1,1)-mode) of 63 kHz. This is at variance with our findings (7 MPa and 23.4 kHz) and more investigations are needed to obtain a better understanding of the tensile stress development in the

TABLE I. Mechanical characteristics for the mechanical modes.

Mode	Frequency (kHz)	Q-factor (10^6)	$Q \times \nu$ (10^{11})
(2,1)	23.4	0.50	0.12
(3,2)	45.5	0.56	0.25
(4,1)	47.5	0.53	0.25
(4,3)	59.5	2.3	1.4

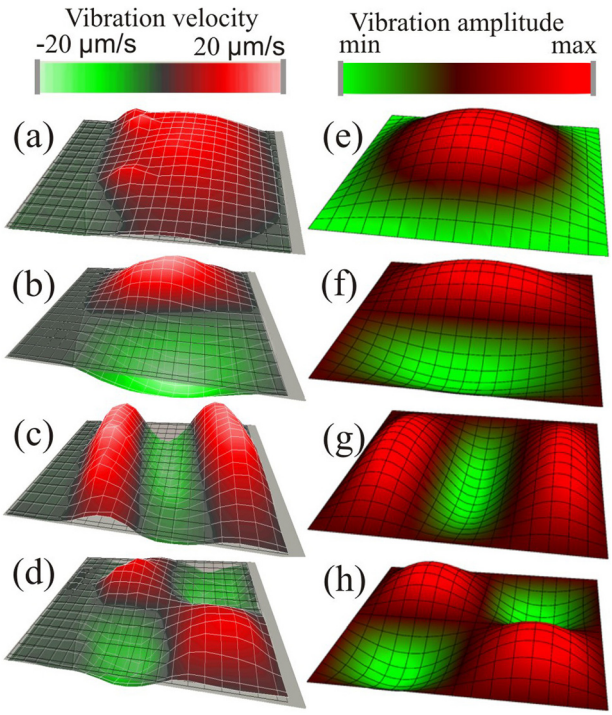

FIG. 3. (Color online) Analysis of the experimental and computed mechanical mode profiles. (a)-(d) Measured deformation profiles of the (1,1), (2,1), (1,3), and (2,2)-mode, respectively, with a micro system analyzer. (e)-(h) Calculated mechanical mode profiles of the (1,1), (2,1), (1,3), and (2,2)-modes, respectively, according to a taut rectangular drumhead model.

fabrication and the relation between the stress and high Q-factors in this system.

In conclusion, we have realized high-Q GaAs nanomembranes with unprecedented sizes for cavity quantum optomechanics experiments. The resonance frequencies and mode profiles are both theoretically and experimentally investigated. Experimental data show good agreement with a simplified model based on a taut rectangular drumhead. The ringdown measurements reveal that the highest Q-factors of the mechanical modes can be up to 2.3×10^6 at room temperature, which underlines the potential of these nanomembranes for cavity cooling experiments. We will report on such studies in a future publication. Further steps can be envisioned by incorporating semiconductor quantum dots in nanomembranes to cool the nanomechanical modes to its ground state[24] and patterning the nanomembranes for controlling of the coupling between phonons and photons.[25]

We gratefully acknowledge S. Schmid and A. Boisen for the assistance of vibration profile measurements and financial support from the Villum Kann Rasmussen Foundation, The Danish Council for Independent Research (Natural Sciences and Technology and Production Sciences), the European Research Council (ERC consolidator grant), and the European project Q-ESSENCE.

[1]J. D. Teufel, T. Donner, D. Li, J. W. Harlow, M. S. Allman, K. Cicak, A. J. Sirois, J. D. Whittaker, K. W. Lehnert, and R. W. Simmonds, Nature **475**, 359 (2011).
[2]J. Chan, T. P. M. Alegre, A. H. Safavi-Naeini, J. T. Hill, A. Krause, S. Gröblacher, M. Aspelmeyer, and O. Painter, Nature **478**, 89 (2011).
[3]D. Vitali, S. Gigan, A. Ferreira, H. R. Böhm, P. Tombesi, A. Guerreiro, V. Vedral, A. Zeilinger, and M. Aspelmeyer, Phys. Rev. Lett. **98**, 030405 (2007).
[4]K. Hammerer, M. Aspelmeyer, E. S. Polzik, and P. Zoller, Phys. Rev. Lett. **102**, 020501 (2009).
[5]T. J. Kippenberg and K. J. Vahala, Science, **321**, 1172 (2008).
[6]F. Marquardt and S. Girvin, Physics **2**, 40 (2009).
[7]I. Favero and K. Karrai, Nature Photon. **3**, 201 (2009).
[8]H. Ukita, Y. Uenishi, and H. Tanaka, Science **260**, 786 (1993).
[9]S. C. Masmanidis, R. B. Karabalin, I. De Vlaminck, G. Borghs, M. R. Freeman, and M. L. Roukes, Science **317**, 780 (2007).
[10]M. Sheik-Bahae and R. I. Epstein, Nature Photon. **1**, 693 (2007).
[11]T. Yoshie, A. Scherer, J. Hendrickson, G. Khitrova, H. M. Gibbs, G. Rupper, C. Ell, O. B. Shchekin, and D. G. Deppe, Nature **432**, 200 (2004).
[12]G. D. Cole, S. Gröblacher, K. Gugler, S. Gigan, and M. Aspelmeyer, Appl. Phys. Lett. **92**, 261108 (2008).
[13]G. D. Cole, Y. Bai, M. Aspelmeyer, and E. A. Fitzgerald, Appl. Phys. Lett. **96**, 261102 (2010).
[14]H. Yamaguchi, K. Kato, Y. Nakai, K. Onomitsu, S. Warisawa, and S. Ishihara, Appl. Phys. Lett. **92**, 251913 (2008).
[15]L. Midolo, P. J. van Veldhoven, M. A. Dündar, R. Nötzel, and A. Fiore, Appl. Phys. Lett. **98**, 211120 (2011).
[16]L. Ding, C. Baker, P. Senellart, A. Lemaitre, S. Ducci, G. Leo, and I. Favero, Phys. Rev. Lett. **105**, 263903 (2010).
[17]L. Ding, C. Baker, P. Senellart, A. Lemaitre, S. Ducci, G. Leo, and I. Favero, Appl. Phys. Lett. **98**, 113108 (2011).
[18]E. Gavartin, R. Braive, I. Sagnes, O. Arcizet, A. Beveratos, T. J. Kippenberg, and I. Robert-Philip, Phys. Rev. Lett. **106**, 203902 (2011).
[19]J.-H. Kim, D. H. Lim, and G. M. Yang J. Vac. Sci. Technol. B **16**, 558 (1998).
[20]E. Yablonovitch, T. Gmitter, J. P. Harbison, and R. Bhat, Appl. Phys. Lett. **51**, 2222 (1987).
[21]U. K. Khankhoje, S.-H. Kim, B. C. Richards, J. Hendrickson, J. Sweet, J. D. Olitzky, G. Khitrova, H. M. Gibbs, and A. Scherer, Nanotechnology **21**, 065202 (2010).
[22]D. J. Wilson, C. A. Regal, S. B. Papp, and H. J. Kimble, Phys. Rev. Lett. **103**, 207204 (2009).
[23]K. Hjort, F. Ericson, J.-Å Schweitz, C. Hallin, and E. Janzén, Thin Solid Films **250**, 157 (1994).
[24]I. Wilson-Rae, P. Zoller, and A. Imamoğlu, Phys. Rev. Lett. **92**, 075507 (2004).
[25]T. P. M. Alegre, A. Safavi-Naeini, M. Winger, and O. Painter, Opt. Express **19**, 5658 (2011).